Quantum Machine Learning over Infinite Dimensions

Hoi-Kwan Lau,[1] Raphael Pooser,[2,3] George Siopsis,[3,*] and Christian Weedbrook[4]
[1]Institute of Theoretical Physics, Ulm University, Albert-Einstein-Allee 11, 89069 Ulm, Germany
[2]Quantum Information Science Group, Oak Ridge National Laboratory, Oak Ridge, Tennessee 37831, USA
[3]Department of Physics and Astronomy, The University of Tennessee, Knoxville, Tennessee 37996-1200, USA
[4]Xanadu, 10 Dundas Street East, Toronto, M5B 2G9, Canada
(Received 20 March 2016; published 21 February 2017)

Machine learning is a fascinating and exciting field within computer science. Recently, this excitement has been transferred to the quantum information realm. Currently, all proposals for the quantum version of machine learning utilize the finite-dimensional substrate of discrete variables. Here we generalize quantum machine learning to the more complex, but still remarkably practical, infinite-dimensional systems. We present the critical subroutines of quantum machine learning algorithms for an all-photonic continuous-variable quantum computer that can lead to exponential speedups in situations where classical algorithms scale polynomially. Finally, we also map out an experimental implementation which can be used as a blueprint for future photonic demonstrations.

DOI: 10.1103/PhysRevLett.118.080501

Introduction.—We are now in the age of big data [1], an unprecedented era in history where storing, managing, and manipulation of information is no longer effective using previously techniques. To compensate for this, one important approach in manipulating such large data sets and extracting worthwhile inferences is by utilizing machine learning techniques. Machine learning [2,3] involves using specially tailored "learning algorithms" to make important predictions in fields as varied as finance, business, fraud detection, and counterterrorism. Tasks in machine learning can involve either supervised or unsupervised learning and can solve such problems as pattern and speech recognition, classification, and clustering. Interestingly enough, the overwhelming rush of big data in the past decade has also been responsible for the recent advances in the closely related field of artificial intelligence [4].

Another important field in information processing which has also seen a significant increase in interest in the past decade is that of quantum computing [5]. Quantum computers are expected to be able to perform certain computations much faster than any classical computer. In fact, quantum algorithms have been developed which are exponentially faster than their classical counterparts [6,7]. Recently, a new subfield within quantum information has emerged combining ideas from quantum computing with artificial intelligence to form quantum machine learning [8].

These discrete-variable schemes have observed a performance that scales logarithmically in the vector dimension, such as supervised and unsupervised learning [9], support vector machine [10], cluster assignment [11], and others [12–18]. Initial proof-of-principle experimental demonstrations have also been performed [19–22]. It was mentioned in Ref. [23] that certain caveats apply to quantum machine learning. However, since then, these caveats (relating to sparsity, condition number, epsilon precision, and quantum output) have been closed or applications found where they are not a concern; cf. [8,10,18,24].

In this Letter, we have developed learning algorithms based on a different, but equally important, type of substrate in quantum computing, those of continuous variables (CVs) [25,26]. A CV system is characterized by having an infinite-dimensional Hilbert space described by measuring variables with a continuous eigenspectra. The year 1999 saw the first important attempt at developing a CV model of quantum computing [27]. Seven years later, the cluster state version [28] of CVs [29,30] accelerated the field due to experimental interest. The result were proof-of-principle demonstrations [31–34], which culminated in a time domain one-million-node cluster [35,36] and a 60-node frequency domain cluster [37]. Further important theoretical work was also carried out [38–47], including an important CV architecture that was fault tolerant [48].

Here, we take advantage of the practical benefits of CVs (high-efficiency room-temperature detectors, broad bandwidths, and large-scale entanglement generation) by generalizing quantum machine learning to the infinite dimension. Specifically, we develop the important CV tools and subroutines that form the basis of the quantum speedup. This includes matrix inversion, principal component analysis, and vector distance. Furthermore, each of these crucial subroutines are given a finite squeezing analysis for future experimental demonstrations along with a suggested photonic implementation.

Quantum machine learning for continuous variables.—The general quantum state of an n-mode system is given by $|f\rangle = \int f(q_1, \ldots, q_n)|q_1\rangle \otimes \ldots |q_n\rangle dq_1 \ldots dq_n$. If we use this state to encode a discrete set of classical data, $\mathbf{a} \equiv \{a_x; x = 1, \ldots, N\}$, which requires at least N classical memory cells, only $n = \log_d N$ modes are sufficient, i.e.,

$$f_{\mathbf{a}}(q_1,\ldots,q_n)=\sum_{x=1}^{N}a_x\prod_{i=1}^{n}\psi_{x_i}(q_i), \tag{1}$$

where d is the number of basis states in each mode; $x=(x_1x_2\ldots x_n)$ is a d-nary representation of x; $\psi_j(q)\equiv\langle q|\psi_j\rangle$ for $j=1,\ldots,d$ is the wave function of the jth single mode basis state, $|\psi_j\rangle$. Here we assume the vector $\mathbf{a}$ is normalized.

Obtaining the classical value of each data a_x still requires $\mathcal{O}(N)$ copies of $|f_{\mathbf{a}}\rangle$. Nevertheless, in some applications only the global behavior of the data set is interesting. For example, the value $\langle f_{\mathbf{a}}|\hat{F}|f_{\mathbf{a}}\rangle$ can be computed efficiently by a quantum computer with significantly fewer copies of $|f_{\mathbf{a}}\rangle$ [23]. Quantum machine learning algorithms take advantage of this property to reduce the amount of memory and operations needed.

If the data set $\mathbf{a}$ is sufficiently uniform, it is known that $|f_{\mathbf{a}}\rangle$ can be efficiently generated. As an illustration, we outline in Supplemental Material [49] an explicit protocol to generate a state with $d=2$ coherent basis states, $|\psi_1\rangle=|\alpha\rangle$, and $|\psi_2\rangle=|-\alpha\rangle$. Our protocol generalizes the discrete variable method in Ref. [50] to CV systems by utilizing the CV implementation of the Grover operator, $e^{i\phi|\psi\rangle\langle\psi|}$ for any given $|\psi\rangle$, as well as the efficient generation of cat states and coherent states [51].

The encoding state construction of general nonuniform data could be constructed by extending the discrete-variable quantum RAM (qRAM) [52] to a CV system or by using a hybrid scheme [53], although the state generation efficiency of such a general encoded state remains an open question [23,54]. Nevertheless, the versatility of CV machine learning is not limited to processing classical data sets that involve a discrete number of data. In the context of universal CV quantum computation, the output of a computer is a CV state that evolves under an engineered Hamiltonian [27]; the wave function of such a full CV output cannot be expressed in the form of Eq. (1). As we will see, the CV machine learning subroutines are capable of processing even full CV states and, therefore, have certain problems that they are more suited to than qubits [55].

In both the data state construction and the quantum machine learning operation, the generalized Grover operator $e^{i\rho' t}$ plays the main role of inducing a phase shift according to an ensemble of unknown given states ρ'. As suggested in Ref. [11], such an operation can be implemented by repeatedly applying the exponential swap operation and tracing out the auxiliary mode, i.e.,

$$\mathrm{tr}_{\rho'}(e^{i\delta t\mathcal{S}}\rho\otimes\rho' e^{-i\delta t\mathcal{S}})=e^{i\delta t\rho'}\rho e^{-i\delta t\rho'}+\mathcal{O}(\delta^2), \tag{2}$$

where by definition the swap operator functions as $\mathcal{S}|\psi_1\rangle|\psi_2\rangle=|\psi_2\rangle|\psi_1\rangle$.

Here we outline the procedure of implementing the exponential operator with standard CV techniques. First of all, we need a qubit as control, which can be implemented by two auxiliary modes 1 and 2, with one and only one photon in both modes; i.e., the state of the modes is $\cos\theta|01\rangle+i\sin\theta|10\rangle$. The rotation angle θ is controllable by applying the rotation operator $R(\theta)\equiv e^{i\theta(\hat{a}_1\hat{a}_2^\dagger+\hat{a}_1^\dagger\hat{a}_2)}$, which can be implemented by linear optics [51]. In addition, we need a controlled-swap operation

$$C_{\mathcal{S}}^{cc'}=e^{-(\pi/4)(\hat{a}_c\hat{a}_{c'}^\dagger-\hat{a}_c^\dagger\hat{a}_{c'})}e^{i\pi\hat{a}_1^\dagger\hat{a}_1\hat{a}_c^\dagger\hat{a}_c}e^{(\pi/4)(\hat{a}_c\hat{a}_{c'}^\dagger-\hat{a}_c^\dagger\hat{a}_{c'})}, \tag{3}$$

which swaps the modes c and c' depending on the photon number of the control qubit. The operations in $C_{\mathcal{S}}^{cc'}$ can be implemented with the quartic gate introduced in Refs. [38,47]. See Supplemental Material [49] for more detail.

The control qubit is first prepared in $|+\rangle\equiv(|01\rangle+|10\rangle)/\sqrt{2}$. By applying the operations in sequence $\exp(i\theta\mathcal{S})=C_{\mathcal{S}}^{cc'}R(\theta)C_{\mathcal{S}}^{cc'}$, the state becomes

$$\begin{aligned}&C_{\mathcal{S}}^{cc'}R(\theta)C_{\mathcal{S}}^{cc'}|+\rangle|\psi\rangle_c|\phi\rangle_{c'}\\&\quad=|+\rangle e^{i\theta\mathcal{S}_{cc'}}|\psi\rangle_c|\phi\rangle_{c'}\\&\quad\equiv|+\rangle(\cos\theta|\psi\rangle_c|\phi\rangle_{c'}+i\sin\theta|\phi\rangle_c|\psi\rangle_{c'}).\end{aligned} \tag{4}$$

The method can be generalized to implement a multimode exponential swap, $\exp(i\theta\mathcal{S}_{cc'}\mathcal{S}_{dd'}\ldots)$, by applying $C_{\mathcal{S}}^{cc'}C_{\mathcal{S}}^{dd'}\ldots R(\theta)C_{\mathcal{S}}^{cc'}C_{\mathcal{S}}^{dd'}\ldots$. We note that the precious resources of a single photon state are not measured or discarded, so it can be reused in future operations.

We emphasize that, in stark contrast to the proposed implementation of the exponential-swap gate in Ref. [11], which is *logical* and thus composed by a series of discrete variable logic gates, our implementation of the exponential-swap gate is *physical*; i.e., it can be applied to full CV states that could not be written as the discrete variable form in Eq. (1). This property allows our subroutine to be applied in, e.g., quantum tomography of CV states, which is more complicated than the discrete variable counterparts due to the large degree of freedom.

CV quantum machine learning algorithms.—We now discuss several key subroutines (matrix inversion, principal component analysis, and vector distance) that power the quantum machine learning problems using the tools we have just introduced.

a. Matrix inversion.—Various machine learning applications involves high-dimensional linear equations, e.g., $\mathbf{A}\mathbf{y}=\mathbf{b}$. The advantage of some quantum machine learning algorithms is the ability to solve linear equations efficiently. Specifically, for any vector $\mathbf{b}=\sum_i b_i\mathbf{e}_i$, computing the solution vector $\mathbf{y}=\mathbf{A}^{-1}\mathbf{b}=\sum_i b_i/\lambda_i\mathbf{e}_i$ is more efficient on a quantum computer [12].

In a CV system, the algorithm starts by preparing the state $|\mathbf{b}\rangle$ and two auxiliary modes in the q quadrature eigenstates, i.e., $|0\rangle_{q,\mathcal{R}}$ and $|0\rangle_{q,\mathcal{S}}$. We apply the operator $\exp(i\delta\gamma\mathbf{A}\hat{p}_{\mathcal{R}}\hat{p}_{\mathcal{S}})$ $1/\delta$ times. Each operator can be implemented based on Eq. (2) and a modified exponential swap gate with the rotation operator in Eq. (4) replaced by the four-mode operator

$$R(\gamma\hat{p}_{\mathcal{R}}\hat{p}_{\mathcal{S}}) = e^{i\gamma\hat{p}_{\mathcal{R}}\hat{p}_{\mathcal{S}}(\hat{a}_1\hat{a}_2^\dagger+\hat{a}_1^\dagger\hat{a}_2)}, \tag{5}$$

which can be implemented efficiently [38]. The state then becomes

$$e^{i\gamma\mathbf{A}\hat{p}_{\mathcal{R}}\hat{p}_{\mathcal{S}}}|\mathbf{b}\rangle|0\rangle_{q,\mathcal{R}}|0\rangle_{q,\mathcal{S}} = \sum_i b_i \int |\mathbf{e}_i\rangle|p\rangle_{p,\mathcal{R}}|\gamma\lambda_i p\rangle_{q,\mathcal{S}}dp, \tag{6}$$

where we have neglected a normalization constant. If the $\mathcal{S}$ auxiliary mode is measured in the q quadrature with outcome $q_{\mathcal{S}}$, then we get

$$\sum_i b_i/\lambda_i|\mathbf{e}_i\rangle|q_{\mathcal{S}}/\gamma\lambda_i\rangle_{p,\mathcal{R}}. \tag{7}$$

Up to the normalization, the solution state $|\mathbf{y}\rangle = \sum_i b_i/\lambda_i|\mathbf{e}_i\rangle$ is obtained if the $\mathcal{R}$ auxiliary mode is measured in the q quadrature, and we get the result $q_{\mathcal{R}} = 0$.

In the infinitely squeezed case, in which the operation is errorless, the successful rate of the last measurement is vanishing. In practice, however, we can employ squeezed vacuum states as auxiliary modes if we permit a small error ϵ. The successful rate of obtaining an answer state then scales as $\mathcal{O}(\epsilon^{3/2})$, which is comparable to the discrete-variable algorithm that has success which scales as $\mathcal{O}(\epsilon)$ [10]. The detailed argument is shown in Supplemental Material [49].

b. Principal component analysis.—The next problem is to find the eigenvalue λ corresponding to a unit eigenvector $\mathbf{e}_i$ with respect to the matrix $\mathbf{A}$, i.e., $\mathbf{A}\mathbf{e}_i = \lambda_i\mathbf{e}_i$. This problem is ubiquitous in science and engineering and can also be used in quantum tomography, supervised learning, and cluster assignment.

The algorithm starts from a data state $|\mathbf{e}_i\rangle$ and an auxiliary mode $\mathcal{R}$ prepared as the zero eigenstate of the q quadrature, $|0\rangle_{q,\mathcal{R}}$. The idea of the algorithm is to apply the operator $e^{i\gamma\mathbf{A}\hat{p}_{\mathcal{R}}}$ that displaces the auxiliary mode according to the eigenvalue, i.e.,

$$e^{i\gamma\mathbf{A}\hat{p}_{\mathcal{R}}}|\mathbf{e}_i\rangle|0\rangle_{q,\mathcal{R}} = |\mathbf{e}_i\rangle e^{i\gamma\lambda_i\hat{p}_{\mathcal{R}}}|0\rangle_{q,\mathcal{R}} = |\mathbf{e}_i\rangle|\gamma\lambda_i\rangle_{q,\mathcal{R}}, \tag{8}$$

and then the eigenvalue can be obtained by measuring the auxiliary mode with homodyne detection. This operator can be implemented by preparing an ensemble such that the density matrix is $\rho' = \mathbf{A}/\mathrm{tr}\mathbf{A}$ and repeatedly applying the techniques in Eq. (2) to implement $e^{i\delta\mathbf{A}\hat{p}_{\mathcal{R}}}$, for $\gamma\mathrm{tr}\mathbf{A}/\delta$ times. Here the argument of the exponential swap operator is not a c number but an operator $\hat{p}_{\mathcal{R}}$. This can be implemented by replacing the rotation operator in Eq. (4) by the three-mode operator

$$R(\hat{p}_R) = e^{i\delta\hat{p}_{\mathcal{R}}(\hat{a}_1\hat{a}_2^\dagger+\hat{a}_1^\dagger\hat{a}_2)}, \tag{9}$$

which can be efficiently implemented by a cubic phase gate and linear optics [27,38].

In practice, the success of the algorithm relies on the distinguishability of $|\gamma\lambda_i\rangle_q$, which depends on the spectrum of eigenvalues, the degree of squeezing s of the auxiliary state, and the magnitude of the error. In Supplemental Material [49], we have shown that $\mathcal{O}(1/\epsilon)$ operations are needed for an error $\epsilon \lesssim 1/(\gamma^2 s)$.

c. Vector distance.—In supervised machine learning, new data are categorized into groups by their similarity to the previous data. For example, the belonging category of a vector $\mathbf{u}$ is determined by the distance D to the average value of the previous data $\{\mathbf{v}_i\}$. The objective of a quantum machine learning algorithm is to compute the value $D^2 \equiv |\mathbf{u} - \sum_{i=1}^M \mathbf{v}_i/M|^2$.

Following the approach given in Ref. [10], we assume an oracle can generate the state

$$|\Psi\rangle = \frac{1}{\mathcal{N}}\left(|\mathbf{u}||0\rangle_I|\tilde{\mathbf{u}}\rangle + \frac{1}{\sqrt{M}}\sum_{i=i}^{M}|\mathbf{v}_i||i\rangle_I|\tilde{\mathbf{v}}_i\rangle\right), \tag{10}$$

where the first mode is denoted as the index mode I; the normalization $\mathcal{N} \equiv \sqrt{|\mathbf{u}|^2 + \sum_i|\mathbf{v}_i|^2/M}$ is supposed to be known. D^2 can be obtained by conducting a swap test on the index mode with a reference mode prepared as $|\Phi\rangle_{\mathcal{R}} \equiv (|0\rangle_{\mathcal{R}} - \sum_{i=1}^M |i\rangle_{\mathcal{R}}/\sqrt{M})/\sqrt{2}$. Various swap tests for CV systems have been proposed where the result is obtained from a photon number measurement [56,57]. Here we propose a swap test that employs only homodyne detection and an exponential swap operation.

We consider two test modes that are prepared in the coherent states $|\beta\rangle_1|0\rangle_2$. The operator $\exp[i(\pi/4)\mathcal{S}_{12}\mathcal{S}_{I\mathcal{R}}]$ is applied to exponential swap the two test modes, as well as the reference and the index modes. After that, the test modes pass through a 50/50 beam splitter. The density operator of the test modes after tracing out the other modes becomes

$$\begin{aligned}\rho_{12} = \frac{1}{2}\Bigg(&\left|\frac{\beta}{\sqrt{2}}\right\rangle_{11}\left\langle\frac{\beta}{\sqrt{2}}\right| + iD^2\left|\frac{\beta}{\sqrt{2}}\right\rangle_{11}\left\langle\frac{-\beta}{\sqrt{2}}\right| \\ &- iD^2\left|\frac{-\beta}{\sqrt{2}}\right\rangle_{11}\left\langle\frac{\beta}{\sqrt{2}}\right| + \left|\frac{-\beta}{\sqrt{2}}\right\rangle_{11}\left\langle\frac{-\beta}{\sqrt{2}}\right|\Bigg)\otimes\left|\frac{\beta}{\sqrt{2}}\right\rangle_{22}\left\langle\frac{\beta}{\sqrt{2}}\right|.\end{aligned} \tag{11}$$

We find that if the 1 mode is homodyne detected in the p quadrature and $\beta \gtrsim 4$, the probability difference of measuring a positive and negative outcome scales as D^2, where the scaling constant is at the order of 0.1 for a wide range of β. See Supplemental Material [49] for further details.

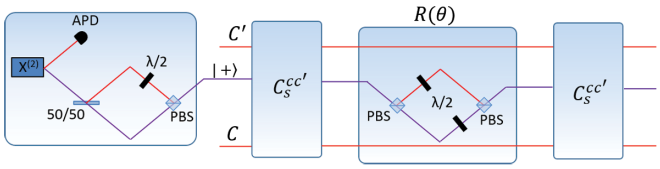

FIG. 1. All-photonic implementation schematic of the operator $\exp(i\theta\mathcal{S}) = C_S^{cc'}R(\theta)C_S^{cc'}$. We initially have an ancillary input mode $|+\rangle = (|01\rangle + |10\rangle)/\sqrt{2}$ with two (swap) modes C and C' used to implement the operators given in Eq. (4). The method for generating $|+\rangle$ is one of many possibilities, e.g., preparing a heralded superposition of polarization states is illustrated. $\chi^{(2)}$, nonlinear crystal source; APD, avalanche photodiode detector; 50/50, balanced beam splitter; $\lambda/2$, half wave plate; PBS, polarizing beam splitter; $C_S^{CC'}$, controlled-swap operator; $R(\theta)$, rotation operator; see the text for an explanation of the operators. Note that $C_S^{cc'}$ can be implemented with the quartic gate [38,47] and $R(\theta)$ can be efficiently implemented using linear optics.

All-photonic implementation.—We outline an all-photonic implementation of the previously mentioned machine learning algorithms. First, one must create an ancillary state for use in the exponential swap gate. One method is to provide a heralded ancilla via parametric down-conversion (see, for example, [51], for a background). The undetected photon is interfered with the vacuum on a 50/50 beam splitter in order to place it in the superposition required for Eq. (4) (see Fig. 1). This serves as an input to the phase-dependent gates outlined in Ref. [38], which can be used to construct the exponential swap gate. The rotation gate in Eq. (4) is essentially the interference of the two modes on a variable reflectivity, or programmable beam splitter, which can be achieved via polarization control and a polarizing beam splitter or via a collection of phase or amplitude modulators. Inverse phase-dependent gate operations are implemented after the rotation.

Each algorithm essentially utilizes a variation of this configuration, in addition to the possibility of a squeezed ancilla in order to increase the accuracy of the result. The principal component analysis problem replaces the variable beam splitter in the swap gate with a two-mode quantum-nondemolition phase gate. It can be implemented by treating the auxiliary mode $\mathcal{R}$ as the ancilla in the phase-dependent gate. Thus, the principal component analysis problem essentially relies on repeated application of the "repeat-until-success" phase gate [38]. In a realistic scenario, $\mathcal{R}$ is in a single-mode squeezed state with finite squeezing (see Supplemental Material [49]), which is experimentally straightforward using a below-threshold optical parametric amplifier (OPA). Phase-sensitive amplification can also be used. The squeezing parameter can be used to tune the accuracy of the computation. The final homodyne detection is also experimentally straightforward with a local oscillator derived from the pump laser used in the OPA (via a doubling cavity, for instance).

The matrix inversion algorithm is experimentally very similar to the eigenvalue problem. The key difference is the use of an extra auxiliary mode, which can be prepared independently with an additional OPA. The four-mode operator is conceptually similar to the operator in Eq. (6) used in the previous algorithm. Each auxiliary mode serves as an ancilla in the phase-dependent gate, and the algorithm otherwise follows a similar approach to the previous one, with a final homodyne detection step for the amplitude quadrature of each auxiliary mode, with the local oscillators derived from the pumps of each OPA.

Finally, the vector distance algorithm requires use of a swap test, which can be implemented via the application of the exponential swap gate between two auxiliary states (which can be coherent states or squeezed states) and the oracle mode in Eq. (10) [10] and the reference mode. The required homodyne detection of the phase quadrature of the first test mode in a bright coherent state and is again experimentally straightforward.

Discussion.—Our previous all-photonic implementations are difficult to do experimentally but are still within the current reach of the latest technological achievements. For instance, high rates of squeezing are now achievable [58], along with the generation of cat states [59]. However, we note that our scheme is not limited to photonic demonstrations but a variety of substrates, including spin ensemble systems, such as trapped atoms and solid state defect centers [60–63].

We hope that the work presented here will lead to further avenues of research, especially since there has been a substantial increase of results in discrete-variable machine learning [14,64–66]. All of these would be interesting to be generalized to continuous variables as future work. Additionally, adapting our current work into the cluster-state formalism [41] would also be interesting in order to take advantage of state-of-the-art experimental interest and the scalability that continuous variables can provide [36,67]. Furthermore, we note another viable option that uses a "best-of-both-worlds" approach to quantum information processing, i.e., hybrid schemes [53,68,69]. It would be interesting to adapt our scheme presented here to such hybrid architectures.

We thank Patrick Rebentrost and Kevin Marshall for helpful discussions. H.-K. L. acknowledges support from the Croucher Foundation. R. P. performed portions of this work at Oak Ridge National Laboratory, operated by UT-Battelle for the U.S. Department of Energy under Contract No. DE-AC05-00OR22725.

*siopsis@tennessee.edu

[1] http://www.ibm.com/big-data/us/en/.
[2] D. Mackay, *Information Theory, Inference and Learning Algorithms* (Cambridge University Press, Cambridge, 2003).

[3] C. M. Bishop, *Pattern Recognition and Machine Learning* (Springer, New York, 2007).
[4] Y. LeCun, Y. Bengio, and G. Hinton, Nature (London) **521**, 436 (2015).
[5] T. D. Ladd, F. Jelezko, R. Laflamme, Y. Nakamura, C. Monroe, and J. L. O'Brien, Nature (London) **464**, 45 (2010).
[6] P. W. Shor, SIAM J. Sci. Statist. Comput. **26**, 1484 (1997).
[7] S. Lloyd, Science **273**, 1073 (1996).
[8] J. Biamonte, P. Wittek, N. Pancotti, P. Rebentrost, N. Wiebe, and S. Lloyd, arXiv:1611.09347.
[9] S. Lloyd, M. Mohseni, and P. Rebentrost, arXiv:1307.0411.
[10] P. Rebentrost, M. Mohseni, and S. Lloyd, Phys. Rev. Lett. **113**, 130503 (2014).
[11] S. Lloyd, M. Mohseni, and P. Rebentrost, Nat. Phys. **10**, 631 (2014).
[12] A. W. Harrow, A. Hassidim, and S. Lloyd, Phys. Rev. Lett. **103**, 150502 (2009).
[13] K. L. Pudenz and D. A. Lidar, Quantum Inf. Process. **12**, 2027 (2013).
[14] N. Wiebe, A. Kapoor, and K. Svore, Quantum Inf. Comput. **15**, 0316 (2015).
[15] Z. Zhao, J. K. Fitzsimons, and J. F. Fitzsimons, arXiv:1512.03929.
[16] P. Rebentrost, M. Schuld, F. Petruccione, and S. Lloyd, arXiv:1612.01789.
[17] A. Steffens, P. Rebentrost, I. Marvian, J. Eisert, and S. Lloyd, arXiv:1609.08170.
[18] P. Rebentrost, A. Steffens, and S. Lloyd, arXiv:1607.05404.
[19] X.-D. Cai, C. Weedbrook, Z.-E. Su, M.-C. Chen, M. Gu, M.-J. Zhu, L. Li, N.-L. Liu, C.-Y. Lu, and J.-W. Pan, Phys. Rev. Lett. **110**, 230501 (2013).
[20] S. Barz, I. Kassal, M. Ringbauer, Y. O. Lipp, B. Dakić, A. Aspuru-Guzik, and P. Walther, Sci. Rep. **4**, 6115 (2014).
[21] X.-D. Cai, D. Wu, Z.-E. Su, M.-C. Chen, X.-L. Wang, Li Li, N.-L. Liu, C.-Y. Lu, and J.-W. Pan, Phys. Rev. Lett. **114**, 110504 (2015).
[22] Z. Li, X. Liu, N. Xu, and J. Du, Phys. Rev. Lett. **114**, 140504 (2015).
[23] S. Aaronson, Nat. Phys. **11**, 291 (2015).
[24] A. M. Childs, R. Kothari, and R. D. Somma, arXiv:1511.02306.
[25] S. L. Braunstein and P. van Loock, Rev. Mod. Phys. **77**, 513 (2005).
[26] C. Weedbrook, S. Pirandola, R. García-Patrón, N. J. Cerf, T. C. Ralph, J. H. Shapiro, and S. Lloyd, Rev. Mod. Phys. **84**, 621 (2012).
[27] S. Lloyd and S. L. Braunstein, Phys. Rev. Lett. **82**, 1784 (1999).
[28] R. Raussendorf and H. J. Briegel, Phys. Rev. Lett. **86**, 5188 (2001).
[29] J. Zhang and S. L. Braunstein, Phys. Rev. A **73**, 032318 (2006).
[30] N. C. Menicucci, Peter van Loock, Mile Gu, Christian Weedbrook, Timothy C. Ralph, and Michael A. Nielsen, Phys. Rev. Lett. **97**, 110501 (2006).
[31] S. Yokoyama, R. Ukai, S. C. Armstrong, J.-i. Yoshikawa, P. van Loock, and A. Furusawa, Phys. Rev. A **92**, 032304 (2015).
[32] K. Miyata, H. Ogawa, P. Marek, R. Filip, H. Yonezawa, J.-i. Yoshikawa, and A. Furusawa, Phys. Rev. A **90**, 060302(R) (2014).
[33] M. Pysher, Y. Miwa, R. Shahrokhshahi, R. Bloomer, and O. Pfister, Phys. Rev. Lett. **107**, 030505 (2011).
[34] S. Takeda, T. Mizuta, M. Fuwa, J.-i. Yoshikawa, H. Yonezawa, and A. Furusawa, Phys. Rev. A **87**, 043803 (2013).
[35] J.-i. Yoshikawa, S. Yokoyama, T. Kaji, C. Sornphiphatphong, Y. Shiozawa, K. Makino, and A. Furusawa, APL Photonics **1**, 060801 (2016).
[36] S. Yokoyama, R. Ukai, S. C. Armstrong, C. Sornphiphatphong, T. Kaji, S. Suzuki, J.-i. Yoshikawa, H. Yonezawa, N. C. Menicucci, and A. Furusawa, Nat. Photonics **7**, 982 (2013).
[37] M. Chen, N. C. Menicucci, and O. Pfister, Phys. Rev. Lett. **112**, 120505 (2014).
[38] K. Marshall, R. Pooser, G. Siopsis, and C. Weedbrook, Phys. Rev. A **91**, 032321 (2015).
[39] H.-K. Lau and C. Weedbrook, Phys. Rev. A **88**, 042313 (2013).
[40] P. van Loock, C. Weedbrook, and M. Gu, Phys. Rev. A **76**, 032321 (2007).
[41] M. Gu, C. Weedbrook, N. C. Menicucci, T. C. Ralph, and P. van Loock, Phys. Rev. A **79**, 062318 (2009).
[42] R. N. Alexander, S. C. Armstrong, R. Ukai, and N. C. Menicucci, Phys. Rev. A **90**, 062324 (2014).
[43] T. F. Demarie, T. Linjordet, N. C. Menicucci, and G. K. Brennen, New J. Phys. **16**, 085011 (2014).
[44] N. C. Menicucci, T. F. Demarie, and G. K. Brennen, arXiv:1503.00717.
[45] P. Wang, M. Chen, N. C. Menicucci, and O. Pfister, Phys. Rev. A **90**, 032325 (2014).
[46] N. C. Menicucci, Phys. Rev. A **83**, 062314 (2011).
[47] K. Marshall, R. Pooser, G. Siopsis, and C. Weedbrook, Phys. Rev. A **92**, 063825 (2015).
[48] N. C. Menicucci, Phys. Rev. Lett. **112**, 120504 (2014).
[49] See Supplemental Material at http://link.aps.org/supplemental/10.1103/PhysRevLett.118.080501 for details on encoding efficiency, non-gaussian gates, and realistic implementation of quantum algorithms.
[50] A. N. Soklakov and R. Schack, Phys. Rev. A **73**, 012307 (2006).
[51] A. Furusawa and P. van Loock, *Quantum Teleportation and Entanglement: A Hybrid Approach to Optical Quantum Information Processing* (Wiley-VCH, New York, 2011).
[52] V. Giovannetti, S. Lloyd, and L. Maccone, Phys. Rev. Lett. **100**, 160501 (2008).
[53] U. L. Andersen, J. S. Neergaard-Nielsen, P. van Loock, and A. Furusawa, Nat. Phys. **11**, 713 (2015).
[54] qRAM is not necessary for every machine learning algorithm, e.g., principal component analysis. In such a case, we need only multiple copies of a density matrix ρ and the possibility to perform controlled swap operations. qRAM can be used to prepare the ρ's, but so can other quantum subroutines.
[55] Recently, we explored in Ref. [47] an algorithm where a CV quantum computer was used to simulate quantum field theory equations where the fields themselves are of a continuous nature.
[56] R. Filip, Phys. Rev. A **65**, 062320 (2002).
[57] H. Jeong, C. Noh, S. Bae, D. G. Angelakis, and T. C. Ralph, J. Opt. Soc. Am. B **31**, 3057 (2014).

[58] H. Vahlbruch, M. Mehmet, K. Danzmann, and R. Schnabel, Phys. Rev. Lett. **117**, 110801 (2016).
[59] W.-B. Gao, C.-Y. Lu, X.-C. Yao, P. Xu, O. Gühne, A. Goebel, Y.-A. Chen, C.-Z. Peng, Z.-B. Chen, and J.-W. Pan, Nat. Phys. **6**, 331 (2010).
[60] J. P. Dowling, G. S. Agarwal, and W. P. Schleich, Phys. Rev. A **49**, 4101 (1994).
[61] K. Tordrup, A. Negretti, and K. Molmer, Phys. Rev. Lett. **101**, 040501 (2008).
[62] J. H. Wesenberg, A. Ardavan, G. A. D. Briggs, J. J. L. Morton, R. J. Schoelkopf, D. I. Schuster, and K. Mø lmer, Phys. Rev. Lett. **103**, 070502 (2009).
[63] Y. Kubo *et al.*, Phys. Rev. Lett. **107**, 220501 (2011).
[64] N. Wiebe, A. Kapoor, and K. M. Svore, arXiv:1412.3489.
[65] M. H. Amin, E. Andriyash, J. Rolfe, B. Kulchytskyy, and R. Melko, arXiv:1601.02036.
[66] N. Wiebe, A. Kapoor, and K. M. Svore, arXiv:1602.04799.
[67] In the one-million-node experiment [36], all nodes were resolved and measured carefully. In fact, due to the time domain encoding, one million is simply a starting point and can in fact be scaled up to an arbitrary size. The main challenge would be the storage and manipulation of more and more data. There is no limit to the distinguishably of the modes themselves. In fact, in quantum optics it is hard to place independent optical fields into the same mode and render them indistinguishable. This is why it is easier to make a nondegenerate optical parametric oscillator than a degenerate one.
[68] N. Liu, J. Thompson, C. Weedbrook, S. Lloyd, V. Vedral, M. Gu, and K. Modi, Phys. Rev. A **93**, 052304 (2016).
[69] H.-K. Lau and M. B. Plenio, Phys. Rev. Lett. **117**, 100501 (2016).